

Design of a concurrent tri-band LNA based on composite right/left-handed transmission line resonators

Faycal El Hardouzi, Mohammed Lahsaini, Mustapha Bahich, Badr Nasiri, Younes Achaoui

Department of Physics, Electronics, Communication Systems and Energy Optimization Group, (OPTIMEE), Faculty of Sciences,
Moulay Ismail University, Meknes, Morocco

Article Info

Article history:

Received Dec 3, 2024

Revised May 15, 2025

Accepted May 26, 2025

Keywords:

Composite right left handed
transmission line

Low noise

Low noise amplifier

Multi band

Split ring resonator

ABSTRACT

This article presents a three-band low noise amplifier (LNA) in microstrip technology based on composite right left handed transmission line (CRLH-TL) resonators for multi-band behavior, which has been designed to meet all the criteria that determine the quality of its operation. The transistor used is biased via a transmission line and matched by $\lambda/4$ transformer filters with CRLH-TL type resonators at the output to establish multiband behavior with improved band rejection to suppress unwanted frequencies and interference. The results demonstrate excellent performance at three frequencies: 900 MHz (15.03 dB gain), 2.1 GHz (13.58 dB gain), and 3.5 GHz (12.57 dB gain), with a noise figure below 2 dB and unconditional stability. The size of the proposed amplifier is $73 \times 63 \text{ mm}^2$ in area.

This is an open access article under the [CC BY-SA](#) license.



Corresponding Author:

Faycal El Hardouzi

Department of Physics, Electronics, Communication Systems and Energy Optimization Group
(OPTIMEE), Faculty of Sciences, Moulay Ismail University

Meknes, Morocco

Email: fa.elhardouzi@edu.umi.ac.ma

1. INTRODUCTION

The rapid evolution of wireless communication technologies has enabled the emergence of new standards, such as 4G and 5G, aimed at delivering high-speed voice, data, and multimedia services. These advances, supported by technological progress, meet the growing user demand for reliable and high-performance communications. Modern networks must not only provide extensive coverage but also ensure a smooth transition between different standards (2G, 3G, 4G) to guarantee continuous service quality [1].

In this context, low noise amplifiers (LNAs) play a crucial role in the signal reception chain. Positioned immediately after the antenna, LNAs amplify low-power signals while minimizing additional noise, which is essential to maintain signal quality in multi-standard environments [2]. Designing these amplifiers for multiple frequency bands presents several challenges, particularly due to interference and the need to reject unwanted bands. In response to these challenges, recent research has explored various configurations of multi-band impedance matching networks, often using impedance transformers and wideband filtering techniques [3]-[12].

However, traditional methods for multi-band LNAs tend to become more complex as the number of supported bands increases. They often require numerous localized components and are difficult to implement at higher frequencies. In this study, we propose an innovative approach for a multi-band LNA based on composite right left handed transmission line (CRLH-TL) resonators, which achieve enhanced performance in terms of unwanted band rejection. Unlike conventional methods, our design remains simple and compact,

providing improved rejection of undesired frequencies through controlled spatial arrangement of the resonators and air gap configuration in fused rings [13]-[15].

The proposed LNA operates efficiently at frequencies of 900 MHz, 2.1 GHz, and 3.5 GHz, corresponding to global system for mobile communications (GSM, 2G), universal mobile telecommunications system (UMTS, 3G), and new radio (NR, 5G) communications standards. Its design is based on the ATF-34143 RF transistor, ensuring stable performance and low noise figure, suitable for the requirements of next-generation mobile applications. This approach offers a promising solution for integrating multi-band LNAs into future communication systems, meeting needs for portability, cost efficiency, and spectral efficiency. In addition, metamaterial-based structures like those we have used are applicable across various fields, including microwave devices such as antennas, as well as other advanced applications [16], [17].

2. PROPOSED CRLH-TL RESONATORS

Composite right/left-handed (CRLH) transmission lines are advanced metamaterial structures comprising unit cells that incorporate both capacitive and inductive elements arranged in series and parallel configurations. This configuration enables the propagation of left-handed (LH) modes at certain frequencies due to series capacitance and shunt inductance, while right-handed (RH) modes dominate at higher frequencies owing to series inductance and shunt capacitance. Unlike ideal LH transmission lines, which consist solely of series capacitance and shunt inductance, CRLH lines account for parasitic effects, making them more suitable for practical applications. A distinctive feature of CRLH lines is their ability to support infinite-wavelength propagation at finite, non-zero frequencies, distinguishing them from other structures [18], [19].

This article introduces two resonators that leverage this unique infinite-wavelength property of CRLH lines, known as zeroth-order resonators (ZORs). These resonators exhibit a resonance frequency independent of the physical length of the transmission line, offering enhanced design flexibility for compact devices. The zeroth-order resonance characteristics are analyzed using the dispersion relation of CRLH lines, formulated through Bloch-Floquet theory. Additionally, the paper emphasizes how these resonators exhibit a resonant frequency independent of the physical length of the transmission line, allowing for greater design flexibility. An ideal open or short CRLH-TL resonator with a physical length of l . Resonance occurs when the condition (1) [18], [19]:

$$\beta_n = \frac{n\pi}{l} \quad (n=0, \pm 1, \pm 2, \dots) \quad (1)$$

as β_n represents the phase constant of the CRLH transmission line for the resonance mode n .

A notable feature of Zero-Order Resonators (ZOR) is that their resonance frequency does not depend on the physical length of the transmission line. This allows tuning of the resonance frequency without altering the resonator's size, making them highly versatile for various applications. Besides filtering out unwanted frequencies, these resonators are also essential for impedance matching in specific circuits, adding multifunctional value to microwave system designs [20]. Therefore, CRLH-TL resonators, especially ZOR, unlock new possibilities in RF circuit design by providing innovative solutions that address the increasing demands for miniaturization and performance in modern wireless technologies. These ZOR resonators resonate at ω_{sh} as shown in (2) [18].

$$\omega_{sh} = \frac{1}{\sqrt{L_L C_R}} \quad (2)$$

with

$$L_L = \mu_0 R_m \left(\ln \left(\frac{8R_m}{h+W_a} \right) - 0.5 \right) \quad [20] \quad (3)$$

such as μ_0 is the vacuum permeability, h is the ring height, W_a is the width of the ring, and R_m is the mean radius (Figure 1).

and

$$C_R = \varepsilon_0 \varepsilon_r \frac{D.W_l}{H} \quad [21] \quad (4)$$

here, ε_0 represents the permittivity of vacuum, ε_r denotes the relative permittivity of the substrate, L is the length of the microstrip line, W_l is its width, and H corresponds to the substrate height (Figure 2).

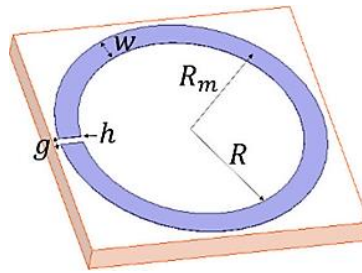


Figure 1. Split ring resonator with geometric parameters

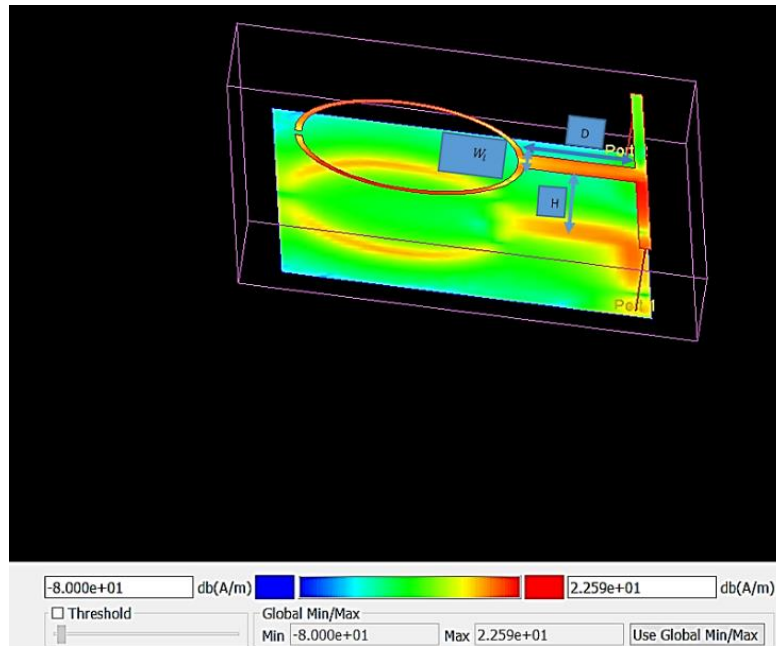


Figure 2. Right-handed side of the split ring resonator with geometric parameters

The circuit shown in Figure 3 achieve resonance at two distinct frequencies, enabling multiband operation. One resonator is tuned to $f = 1.6$ GHz, while the other resonates at $f = 2.8$ GHz. These frequencies were determined using the computer-aided design program advanced design system (ADS). To verify the theoretical cited in (2)-(4) within our circuit, we will examine, for example, the resonator set to resonate at $f = 2.8$ GHz. Table 1 outlines the parameters applied in the design of this specific resonator.



Figure 3. Image of the manufactured prototype of the proposed zero-order resonator

Table 1. Design parameters for the CRLH-TL resonator

μ_0	R_m	R	W_a	h	
12×10^{-7} H/m	4.7 mm	4.35 mm	0.7 mm	35×10^{-3} mm	
ϵ_0	ϵ_r	D	W_l	H	g
8.854×10^{-12} F/m	3.38	2.34 mm	1.6 mm	0.813 mm	0.5 mm

So, the resonant frequency is:

$$f_{res} = \frac{1}{2\pi\sqrt{L_L C_R}} = 2.88 \text{ GHz} \quad (5)$$

This is almost the same result we obtained from simulation, as shown in Figure 4. Following the same steps for the second resonator, we find that $f = 1.58$ GHz. This is almost the same result we obtained through simulation, as shown in Figure 4.

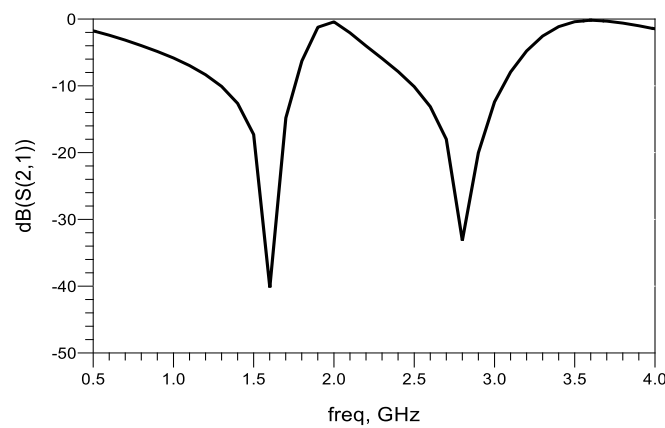


Figure 4. Measured transmittance (S21) of the resonators (Figure 3), highlighting the frequency response, passband, and rejection bands

From Figure 4, we can see that the resonators resonate at frequencies of 1.6 GHz and 2.8 GHz, which are almost the same as the frequencies obtained by applying the previously mentioned (2) to (4). We have dimensioned the two resonators to resonate at these frequencies (1.6 GHz and 2.8 GHz) in order to create bands around 900 MHz, 2.1 GHz, and 3.5 GHz. Thus, these resonators have high precision, and these three bands are now separated from each other, which helps to avoid interference between these bands. From here, the importance of the resonator becomes clear, as does its ease of multi-band realization and high-precision tuning of the desired resonant frequency.

The importance of this resonator in the multiband application can be clearly seen in comparison with other work in the multiband field, thanks to its smooth and controlled control. It also enables us to adjust and widen the rejection band, while remaining extremely compact. The frequency of our system's 0th-order resonator is directly related to the value of the unit cell's capacitor C_R and coil L_L , rather than to the physical length of the resonator. What's more, this resonator requires no localized components, making it easy and cost-effective to manufacture. Its use in our amplifier gives excellent results.

3. PROPOSED LNA TRIBAND

Figures 5 and 6 displays the proposed tri-band LNA. For this design, we employed the ATF34143, a commercially available pseudomorphic HEMT transistor, with bias voltages set to $V_{DS}=4$ V and $V_{GS}=-0.1$ V. The amplifier is constructed on a Roger RO4003 substrate, featuring a relative permittivity of 3.38, a loss tangent of 0.0027, and a thickness of 0.813 mm. The overall dimensions of the amplifier are 73×62 mm². The key contribution of this work centers on the use of resonators to create a multiband response within a LNA structure.

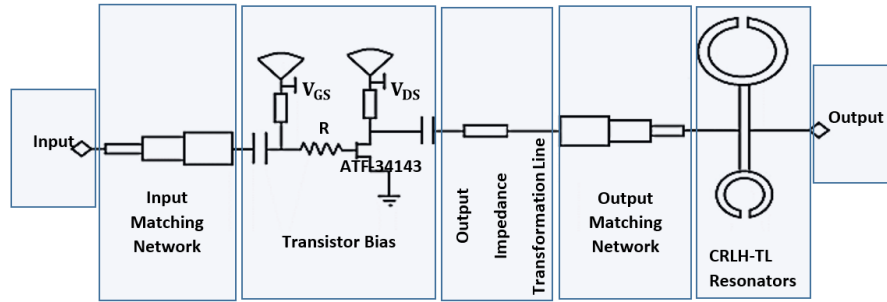


Figure 5. Schematic of the proposed multiband LNA

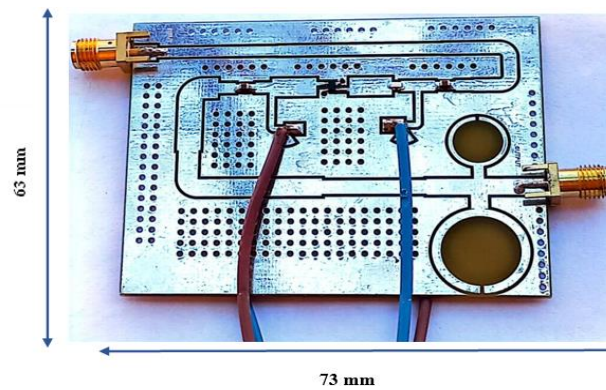


Figure 6. Photograph of the fabricated prototype of the proposed tri-band LNA

The multiband LNA is designed with a calibrated resistor to ensure stability and minimize noise. A DC power supply is used to precisely bias the transistor, which is connected to a series capacitor and a $\lambda/4$ transformer leading to a radial line section. This configuration optimizes the transistor's operating point, improving gain, noise figure, linearity, output power, and expanding the amplifier's bandwidth to process a wider frequency range [22], [23].

Effective impedance matching is also emphasized, as it is vital for the performance of microwave amplifiers. To optimize power transfer and prevent instability, a quarter-wave line is used between load and input impedances. Multi-section designs with cascaded $\lambda/4$ lines and uniform quarter-wave section impedance transformers are implemented to enhance matching further. The formula establishing the relationship between characteristic impedance Z_0 , load impedance Z_L , and Impedance values that define the multi-section transformer is as (6) [23]:

$$\ln \frac{Z_{n+1}}{Z_n} = 2^{-N} C_n^N \ln \frac{Z_L}{Z_0} \quad (6)$$

To perform the matching, we study the case of three sections of length ($\lambda/4$), as shown in Figure 7. This approach aims to ensure optimal impedance matching at both the input and output of the transistor, in order to reduce losses due to reflections. Effective matching directly improves the amplifier's performance, especially in terms of gain and stability.

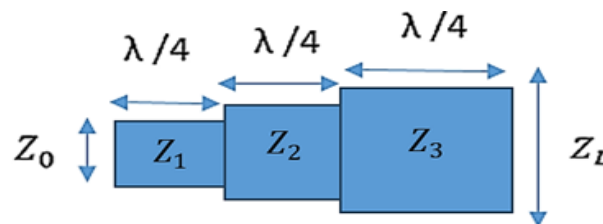


Figure 7. Three-section wave quad transformer

For the 2.2 GHz center frequency, we find: the optimum impedance at the transistor input is $Z_s = 43,89 - j0,14$ and the optimum impedance at the transistor output is $Z_L = 31,93 - j4,96$, so $Z_{in} = 43,89 + j0,14$ and $Z_{out} = 31,93 + j4,96$. As far as CRLH-TL resonators are concerned, we discussed them in section 2.

4. RESULTS AND DISCUSSION

The performance results of our tri-band LNA circuit are presented in Figures 8 to 11. Figure 8 displays the simulated gain S_{21} for the multi-band LNA. As shown, the signal gain reaches 15.03 dB at 900 MHz, 13.58 dB at 2.1 GHz, and 12.57 dB at 3.5 GHz. The reverse isolation S_{12} indicates the internal feedback from the output to the input of the two-port device. The simulated reverse isolation of the proposed multi-band LNA is shown in Figure 7. At 900 MHz, S_{12} is -34 dB, at 2.1 GHz it is -26.19 dB, and at 3.5 GHz it is -20.44 dB. For proper LNA operation, it is crucial to minimize S_{12} . A low reverse isolation ensures maximum isolation between the output and input, which is vital for achieving optimal stability and performance.

Figure 9 presents the reflection coefficients at the input (S_{11}) and output (S_{22}) for low excitation levels. As observed in Figure 9, the input reflection losses are -6.76 dB at 900 MHz, -10.17 dB at 2.1 GHz, and -12.76 dB at 3.5 GHz. For the output, the reflection losses are -1.5 dB at 900 MHz, -6.4 dB at 2.1 GHz, and -11.64 dB at 3.5 GHz.

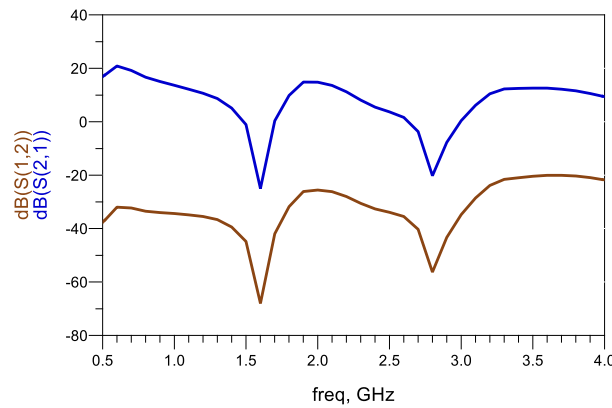


Figure 8. Transmission coefficients S_{21} and S_{12}

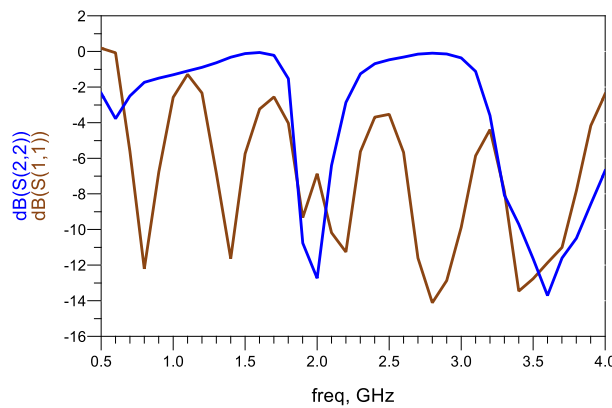


Figure 9. Reflexion coefficients S_{11} and S_{22}

Figure 10 illustrates the evolution of the noise figure as a function of frequency. It can be observed that the minimum noise figure (NFmin) remains below 2 across all targeted frequency bands. This demonstrates that the designed amplifier provides good noise performance, which is essential for ensuring high-quality signal reception.

Figure 11 presents the stability coefficients k (StabFact1) and μ (μ' and μ_1) simulated at the three targeted frequencies. Since the stability factors exceed 1 across all frequency bands, the stability criteria for the proposed multi-band LNA are fulfilled. This ensures that the LNA can handle any source or load at these frequencies without the risk of instability or oscillation. In Table 2, the performance of the designed multiband amplifier is summarized and Compared with the state of the art in multiband amplifiers. We can clearly see that our technique is useful and easy, and despite our single stage, we've achieved good results.

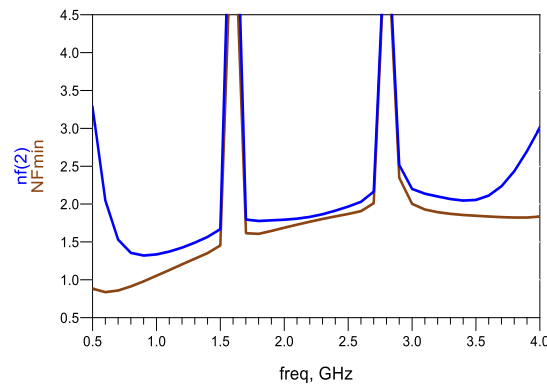


Figure 10. Noise of LNA multiband

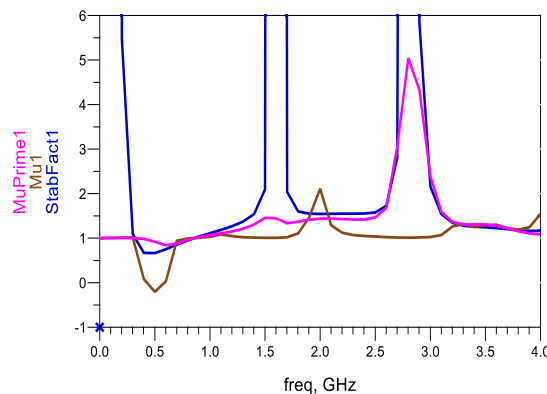


Figure 11. The stability factors of multiband LNA

Table 2. State of the art of low-noise multiband amplifiers

Ref.	Freq.(GHz)	Gain (dB)	S(1,2) (dB)	S(1,1) (dB)	NF (dB)	VDS (V)	Number of stage
[24]	2.44	7.15	-	-10.54	4.34	2.7	Single
	5.25	7.80	-	-15.98	4.69		
[25]	2.45	28.4	-45	-13	0.7	1	Two stage (cascade)
	5.25	28.8	-45	-20	1.1		
[26]	28	16.2	-	-	2.8	-	Cascode topology
	60	15	-	-	3.35		
[This work]	0.9	15.03	-34	-6.7	0.98	4	Single
	2.1	13.58	-26.19	-10.17	1.72		
	3.5	12.57	-20.44	-12.76	1.84		

5. CONCLUSION

This study introduces the design and analysis of a multiband low-noise microwave amplifier based on resonators and implemented in microstrip technology using a composite right/left-handed (CRLH) transmission line. The results indicate that the proposed amplifier delivers excellent performance for mobile network standards including GSM (2G), UMTS (3G), and NR (5G). Specifically, the amplifier achieves a

gain of 15.03 dB with a noise figure of 0.98 at 900 MHz, a gain of 13.58 dB with 1.72 noise at 2.1 GHz, and a gain of 12.57 dB with 1.84 noise at 3.5 GHz, powered by $V_{DS}=4V$ and $V_{GS}=-0.1 V$.

The proposed amplifier demonstrates strong stability, high gain, and low noise, thereby validating the novel application of CRLH-TLs to achieve multiband capabilities in amplifiers. This approach shows promise for broad application across various amplifier types.

FUNDING INFORMATION

We do not receive any funding.

AUTHOR CONTRIBUTIONS STATEMENT

This journal uses the Contributor Roles Taxonomy (CRediT) to recognize individual author contributions, reduce authorship disputes, and facilitate collaboration.

Name of Author	C	M	So	Va	Fo	I	R	D	O	E	Vi	Su	P	Fu
Faycal El Hardouzi	✓	✓	✓	✓	✓		✓	✓	✓	✓				
Mohammed Lahsaini	✓	✓						✓	✓		✓	✓		
Mustapha Bahich		✓	✓	✓						✓	✓			
Badr Nasiri		✓								✓	✓			
Younes Achaoui	✓				✓					✓	✓	✓		

C : **C**onceptualization

M : **M**ethodology

So : **S**oftware

Va : **V**alidation

Fo : **F**ormal analysis

I : **I**nvestigation

R : **R**esources

D : **D**ata Curation

O : Writing - **O**riginal Draft

E : Writing - Review & **E**ditng

Vi : **V**isualization

Su : **S**upervision

P : **P**roject administration

Fu : **F**unding acquisition

CONFLICT OF INTEREST STATEMENT

The authors declare no conflict of interest.

INFORMED CONSENT

We have obtained informed consent from all individuals included in this study, in accordance with legal and ethical requirements for privacy protection.

ETHICAL APPROVAL

This research does not involve human subjects and therefore does not require approval from an ethics committee.

DATA AVAILABILITY

The data availability statement is a valuable link between a paper's results and the supporting Data availability is not applicable to this manuscript, as no new data were created or separately analyzed for this study. The results are available within the article and/or its figures.




REFERENCES

- [1] A. Biswas and V. R. Gupta, "Multiband antenna design for smartphone covering 2G, 3G, 4G and 5G NR frequencies," in *2019 3rd International Conference on Trends in Electronics and Informatics (ICOEI)*, IEEE, Apr. 2019, pp. 84–87. doi: 10.1109/ICOEI.2019.8862713.
- [2] N. Nallam and S. Chatterjee, "Multi-band frequency transformations, matching networks and amplifiers," *IEEE Transactions on Circuits and Systems I: Regular Papers*, vol. 60, no. 6, pp. 1635–1647, Jun. 2013, doi: 10.1109/TCSI.2012.2221175.
- [3] X. Zheng, Y. Liu, S. Li, C. Yu, Z. Wang, and J. Li, "A dual-band impedance transformer using PI-section structure for frequency-dependent complex loads," *Progress In Electromagnetics Research C*, vol. 32, pp. 11–26, 2012, doi: 10.2528/PIERC12052909.
- [4] Y. Liu, Y. Zhao, S. Liu, Y. Zhou, and Y. Chen, "Multi-frequency impedance transformers for frequency-dependent complex loads," *IEEE Transactions on Microwave Theory and Techniques*, vol. 61, no. 9, pp. 3225–3235, Sep. 2013, doi: 10.1109/TMTT.2013.2274779.
- [5] B.-T. Moon and N.-H. Myung, "A dual-band impedance transforming technique with lumped elements for frequency-dependent complex loads," *Progress In Electromagnetics Research*, vol. 136, pp. 123–139, 2013, doi: 10.2528/PIER12111811.




- [6] M. A. Maktoomi, M. S. Hashmi, and F. M. Ghannouchi, "A T-section dual-band matching network for frequency-dependent complex loads incorporating coupled line with DC-block property suitable for dual-band transistor amplifiers," *Progress In Electromagnetics Research C*, vol. 54, pp. 75–84, 2014, doi: 10.2528/PIERC14090403.
- [7] M. A. Maktoomi, R. Gupta, and M. S. Hashmi, "A dual-band impedance transformer for frequency-dependent complex loads incorporating an L-type network," in *2015 Asia-Pacific Microwave Conference (APMC)*, IEEE, Dec. 2015, pp. 1–3. doi: 10.1109/APMC.2015.7411641.
- [8] M. Chuang, "Analytical design of dual-band impedance transformer with additional transmission zero," *IET Microwaves, Antennas & Propagation*, vol. 8, no. 13, pp. 1120–1126, Oct. 2014, doi: 10.1049/iet-map.2014.0181.
- [9] F. Teguh, S. Supriyanto, H. Herudin, W. Gunawan, and A. Mudrik, "Multiband RF low noise amplifier (LNA) base on multi section impedance transformer for multi frequency application," *International Journal of Applied Engineering Research*, vol. 11, no. 5, pp. 3478–3483, 2016.
- [10] J. Lee and C. Nguyen, "A K-/Ka-band concurrent dual-band single-ended input to differential output low-noise amplifier employing a novel transformer feedback dual-band load," *IEEE Transactions on Circuits and Systems I: Regular Papers*, vol. 65, no. 9, pp. 2679–2690, Sep. 2018, doi: 10.1109/TCSI.2018.2830808.
- [11] Z. Wang *et al.*, "A Ka-Band switchable LNA with 2.4-dB NF employing a varactor-based tunable network," *IEEE Microwave and Wireless Components Letters*, vol. 31, no. 4, pp. 385–388, Apr. 2021, doi: 10.1109/LMWC.2021.3059655.
- [12] A. Aneja, X. J. Li, and P. H. J. Chong, "Design and analysis of a 1.1 and 2.4 GHz concurrent dual-band low noise amplifier for multiband radios," *AEU - International Journal of Electronics and Communications*, vol. 134, p. 153654, May 2021, doi: 10.1016/j.aeue.2021.153654.
- [13] R. A. Alahnomi, Z. Zakaria, E. Ruslan, S. R. Ab Rashid, and A. A. Mohd Bahar, "High-Q sensor based on symmetrical split ring resonator with spurlines for solids material detection," *IEEE Sensors Journal*, vol. 17, no. 9, pp. 2766–2775, May 2017, doi: 10.1109/JSEN.2017.2682266.
- [14] C. Soemphol, P. Thitimahatthanagulsol, E. Khoomwong, and M. Kupimai, "Q-factor control in asymmetry single circular split ring resonator via position of gap," in *2017 International Electrical Engineering Congress (iEECON)*, IEEE, Mar. 2017, pp. 1–3. doi: 10.1109/IEECON.2017.8075844.
- [15] Y. -H. Jeng, S.-F. R. Chang, and H. -K. Lin, "A high stopband-rejection LTCC filter with multiple transmission zeros," *IEEE Transactions on Microwave Theory and Techniques*, vol. 54, no. 2, pp. 633–638, Feb. 2006, doi: 10.1109/TMTT.2005.862669.
- [16] S. Liu, Z. Wang and Y. Dong, "Compact Wideband SRR-Inspired Antennas for 5G Microcell Applications," in *IEEE Transactions on Antennas and Propagation*, vol. 69, no. 9, pp. 5998–6003, Sept. 2021, doi: 10.1109/TAP.2021.3070001..
- [17] I. Moumen, M. Elhabchi, M. N. Srifi, and R. Touahni, "Metamaterial inspired circular antenna for Bluetooth band integration," *TELKOMNIKA (Telecommunication Computing Electronics and Control)*, vol. 22, no. 3, p. 510, Jun. 2024, doi: 10.12928/telkomnika.v22i3.25756.
- [18] A. Sanada, C. Caloz, and T. Itoh, "Novel Zeroth order resonance in composite right/left-handed transmission line resonators," in *2003 Asia-Pacific Microwave Conference*, 2003, pp. 1588–1592. doi: 10.1109/TMTT.2003.819151.
- [19] T. Jang, J. Choi, and S. Lim, "Compact coplanar waveguide (CPW)-fed Zeroth-order resonant antennas with extended bandwidth and high efficiency on vialess single layer," *IEEE Transactions on Antennas and Propagation*, vol. 59, no. 2, pp. 363–372, Feb. 2011, doi: 10.1109/TAP.2010.2096191.
- [20] N. Alrayes and M. I. Hussein, "Metamaterial-based sensor design using split ring resonator and Hilbert fractal for biomedical application," *Sensing and Bio-Sensing Research*, vol. 31, Feb. 2021, doi: 10.1016/j.sbsr.2020.100395.
- [21] L. La Spada, F. Bilotti, and L. Vegni, "Metamaterial-based sensor design working in infrared frequency range," *Progress In Electromagnetics Research B*, vol. 34, pp. 205–223, 2011, doi: 10.2528/PIERB11060303.
- [22] I. J. Bahl, *Fundamentals of RF and Microwave Transistor Amplifiers*. Wiley, 2009. doi: 10.1002/9780470462348.
- [23] F. El Hardouzi and M. Lahsaini, "Design of a Broadband LNA Based on Various Distributed-Element Microwave Filters With Semi-Distributed Notch Filtering for Interference Rejection", in *2024 4th International Conference on Innovative Research in Applied Science, Engineering and Technology (IRASET)*, FEZ, Morocco: IEEE, May 2024, pp. 1–6, doi: 10.1109/IRASET60544.2024.10548249.
- [24] B. Iyer and N. P. Pathak, "A concurrent dual-band LNA for noninvasive vital sign detection system," *Microwave and Optical Technology Letters*, vol. 56, no. 2, pp. 391–394, Feb. 2014, doi: 10.1002/mop.28127.
- [25] Z. Ke, S. Mou, K. Ma, and F. Meng, "A 0.7/1.1-dB ultra-low noise dual-band LNA based on SISL platform," *IEEE Transactions on Microwave Theory and Techniques*, vol. 66, no. 10, pp. 4576–4584, Oct. 2018, doi: 10.1109/TMTT.2018.2845363.
- [26] A. A. Nawaz, J. D. Albrecht and A. Çağrı Ulusoy, "A Ka/V Band-Switchable LNA With 2.8/3.4 dB Noise Figure," in *IEEE Microwave and Wireless Components Letters*, vol. 29, no. 10, pp. 662–664, Oct. 2019, doi: 10.1109/LMWC.2019.2939540.

BIOGRAPHIES OF AUTHORS






Faycal El Hardouzi    was born in Sidi Slimane, Morocco, in 1983. He obtained a master's degree in microelectronics from the Université Ibn Tofail, Faculté des Sciences de Kénitra, Morocco, in 2010, and is currently a doctoral student at the Université Moulay Ismail, Faculté des Sciences de Meknès, Morocco. His areas of research include microwave circuits and, more specifically, high-frequency amplifiers. He can be contacted at email: fa.elhardouzi@edu.umi.ac.ma.






Mohammed Lahsaini    is a professor in the Department of Physics at the Faculty of Sciences, Moulay Ismail University, Meknes, Morocco. From his extensive experience in electronic and microwave communication system backgrounds, he has chosen to specialize in microwave engineering. He has co-authored numerous scientific publications and filed several patents dealing with active and metamaterial-based components, through which he actively contributes to microwave technology innovations. His work focuses on improving the performance and energy efficiency of modern communication devices, while also mentoring the next generation of researchers and engineers. He can be contacted at email: mohammed.lahsaini@gmail.com.






Mustapha Bahich    received his Bachelor's degree in Electrical Engineering, Master's degree in Information Processing, and a Doctorate degree in Applied Optics and Information Processing from the University of Hassan II at Casablanca in 2003, 2005, and 2011, respectively. He is currently an associate professor with the Department of Physics, University of Moulay Ismail, Meknes. His research interests include signal and image processing, electronics, and computational physics. He can be contacted at email: m.bahich@umi.ac.ma.



Badr Nasiri    born in Morocco, holds a Ph.D. in Electronics and Telecommunications from the Faculty of Sciences and Techniques at Hassan 1st University in Settat, Morocco. He is currently an Associate Professor of Electronics at the Faculty of Science, Moulay Ismail University in Meknes, Morocco. His research focuses on the design and implementation of both passive and active planar circuits using metamaterials. He can be contacted at email: nasiribadr1988@gmail.com.



Younes Achaoui    received his Ph.D. in Applied Physics from Franche-Comté University at Besançon, France, in 2011. From 2012 to 2018, he served as a postdoctoral research fellow at three different laboratories, namely, the Laboratoire de Mécanique et d'Acoustique, Fresnel Institute, and FEMTO-ST Institute. In 2018, he joined Moulay Ismail University as an assistant professor. Since then, he has co-authored more than 50 papers in peer-reviewed journals and given seminars at various conferences worldwide. His main research activities deal with wave control in the broadest sense of the term. This covers noise insulation and seismic shielding using so-called metamaterials on one hand, and surface plasmon polaritons through photonic and plasmonic crystals on the other. Currently, he is interested in implementing the counter-intuitive functionalities discovered in metamaterials within compact planar microstrip elements, with a view to conceiving unprecedented microwave devices. He can be contacted at email: achauiyounes@hotmail.com.